Commissioning of the Ly-α Pinhole Camera Diagnostic at DIII-D: Towards Inboard and Outboard Neutral Density Measurements

F. M. Laggner[1], A. M. Rosenthal[2], A. Bortolon[1], T. M. Wilks[2],
J. W. Hughes[2], F. Effenberg[1], M. W. Shafer[3], T. Odstrcil[4] and the DIII-D team
[1] *Princeton Plasma Physics Laboratory, Princeton, New Jersey 08543, USA*
[2] *MIT Plasma Science and Fusion Center, Cambridge, Massachusetts 02139, USA*
[3] *Oak Ridge National Laboratory, Oak Ridge, Tennessee 37831, USA*
[4] *General Atomics, P.O. Box 85608, San Diego, California 92186, USA*

Abstract

The absolutely calibrated LLAMA diagnostic (LLAMA is the Lyman-Alpha Measurement Apparatus) has been recently installed on DIII-D [1, 2] to determine the neutral gas density (n_0) profile and thereby, quantify the edge particle source in deuterium plasmas. In the initial diagnostic commissioning, absolutely calibrated Ly-α brightness profiles were measured at the high field side (HFS) and low field side (LFS) in high confinement mode with forward and reversed toroidal magnetic field (B_t) direction. The deuterium n_0 profiles and ionization rate profiles are reconstructed from the inverted Ly-α emissivity profiles, in combination with the electron density (n_e) and electron temperature (T_e) profiles, solving the rate equation system for the deuterium atom occupation density. LLAMA measurements exhibit HFS-LFS asymmetries in pedestal particle source, which depend on the B_t direction highlighting the importance of scrape-off layer (SOL) drift direction and the necessity to consider the full poloidal particle source distribution in edge transport analyses.

Introduction and Motivation

LLAMA is a pinhole camera system that measures the Ly-α brightness across the plasma boundary at the inboard, HFS, and outboard, LFS, plasma edge region [1, 2]. The implementation of the LLAMA builds on experience from previous vacuum ultraviolet (VUV) measurements of the Ly-α line radiation [3, 4], which use AXUV photodiode arrays with Ly-α filters. Figure 1 presents the LLAMA's optical components. Radiation from the plasma enters through a 2 mm by 8 mm rectangular pinhole. The Ly-α-selective Bragg mirror and the bandpass interference filter narrow the incoming spectrum and reject parasitic CIII radiation. A light tight box holds the filter and contains the 20 channel AXUV photodiode detector array. The lines of sight (LOS) are below the midplane, oriented tangentially in the toroidal direction (see figure 1e). Measurements of Ly-α line radiation provide some key advantages compared to more common measurements of the Balmer series (visible part of the spectrum). Surface reflections from carbon plasma facing components are reduced, which can become a substantial issue for Balmer-alpha line (Ba-α) spectroscopy [5], and fewer molecular contributions are expected around the Ly-α line. The responsivity of AXUV detectors suffers significant degradation upon radiation

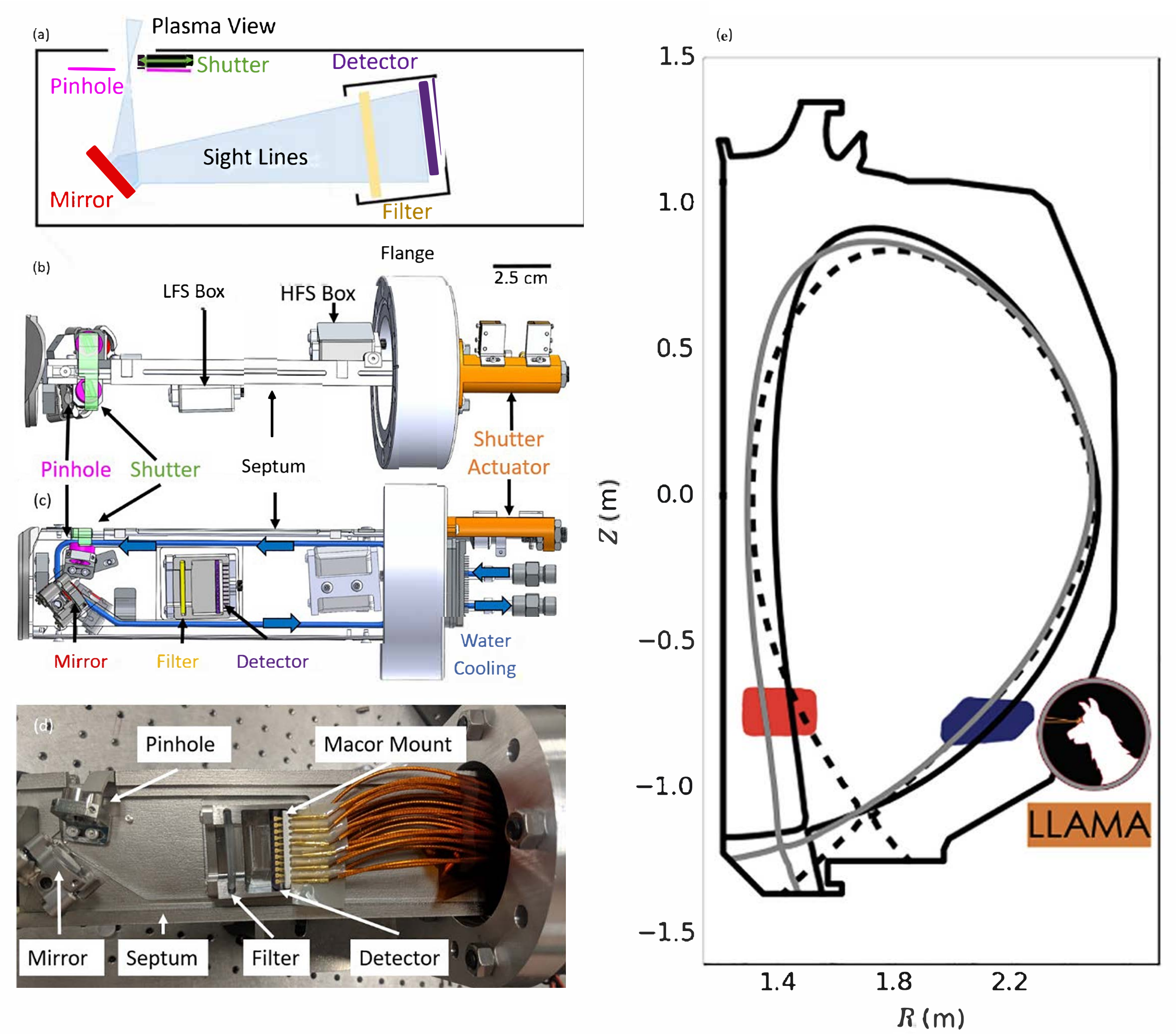

Figure 1: (a) Schematic of the LLAMA's optical components, (b,c) side and top down views of the CAD model, (d) the assembled optical components and (e) LOS on the poloidal cross section and typical separatrix locations. Figure adapted from [1].

exposure [6]. For this reason, a regularly applied calibration procedure using a commercially available VUV source was developed [2].

Absolutely calibrated Ly-α measurements

Figure 2 presents a comparison of radial Ly-α brightness profiles in lower single null (LSN) plasma discharges, which are so-called 'reference plasma discharges' that are regularly repeated to track DIII-D machine conditions throughout campaigns. Reference plasma discharges are performed with forward (Fwd.) and reversed (Rev.) B_t direction, hence, for both directions of the $B \times \nabla B$ and the SOL $E_r \times B$ drifts. The compared plasma discharges have the same shape in lower single null divertor configuration, neutral beam heating power (P_{NBI}) of 4 MW, a plasma current of 1.15 MA and a toroidal magnetic field of ± 2 T. The outermost channel of the LLAMA LFS system has been used to determine and to compensate for electromagnetic noise pickup, since very low Ly-α emission is expected in the far-SOL. In figure 2a, the forward B_t

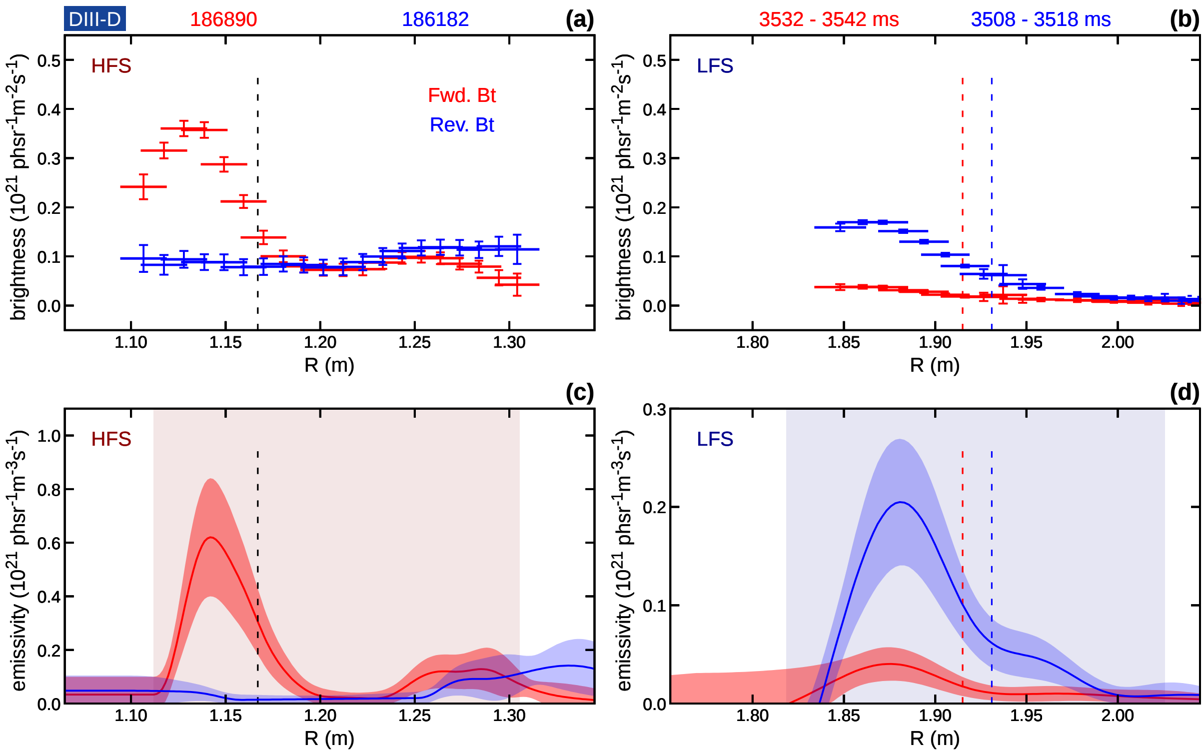

Figure 2: Absolutely calibrated Ly-α brightness profile of a LLAMA measurement in DIII-D (a) on the HFS and (b) on the LFS and (c,d) inverted Ly-α emissivity profiles.

discharge (red), with favorable B × ∇B towards the lower divertor, shows a substantially larger Ly-α emission on the HFS in comparison to the reversed B_t discharge (blue), with unfavorable B × ∇B away from the lower divertor. On the LFS (see figure 2b), the reversed field direction exhibits a higher Ly-α brightness.

Profile inversion and neutral density reconstruction

An optimized tomographic inversion, originally developed for application to a Soft X-ray diagnostic [7], has been adapted and implemented for the LLAMA diagnostic. The inversion uses the Tikhonov regularization with linear computational complexity in the number of basis functions and is combined with the minimum Fisher information to enforce constraints like non-negative emissivity and boundary conditions of zero emissivity at the wall and in the plasma core. Figures 2c and 2d present the inverted Ly-α emissivity profiles. The strong HFS-LFS asymmetries persist with the inversion; however, some artifacts, which likely originate from not properly accounted core radiation, occur on the HFS inside the separatrix (R > 1.25 m). The Ly-α emissivity, n_e and T_e profiles, acquired by the Thomson scattering (TS) diagnostic, serve as input to solve the rate equation system for the deuterium atom occupation density to reconstruct the ionization rate and n_0. For simplicity, the 'corona equilibrium' approximation is employed such that temporal changes or transport for neutrals or plasma are not considered. The analysis uses atomic rate coefficients [8] that are implemented into the Monte Carlo neutral code DEGAS2 [9]. A similar approach has been recently undertaken at NSTX-U to evaluate

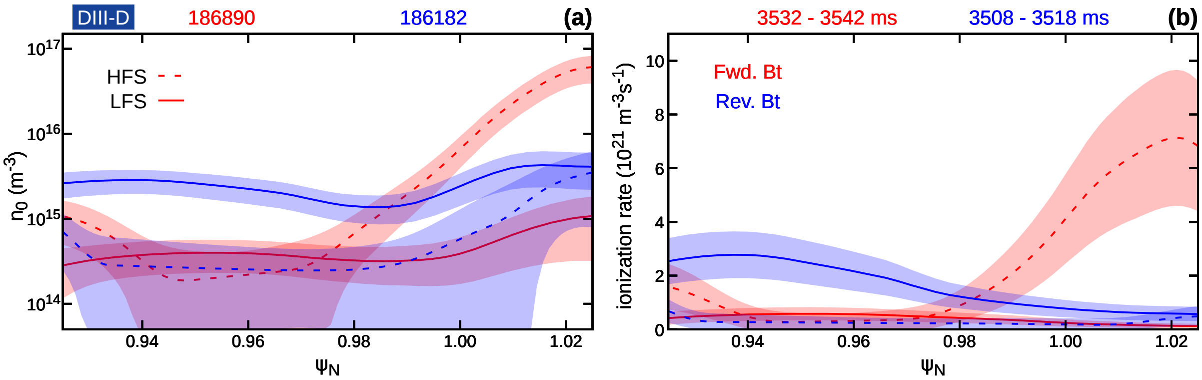

Figure 3: Reconstructed neutral profiles of a LLAMA measurements (a) neutral gas density (n_0) and (b) ionization rate on the HFS (dashed) and LFS (solid).

Ba-α measured by the ENDD diagnostic [10]. The reconstructed neutral densities in figure 3a and ionization rates in figure 3b indicate that the HFS contribution dominates the main chamber fueling of the pedestal region in Fwd. B_t (red, dashed line), while in Rev. B_t the LFS becomes dominant (blue, solid line).

Summary and Outlook

This contribution presents the absolutely calibrated LLAMA diagnostic on DIII-D and a workflow to reconstruct n_0 and ionization profiles from the Ly-α brightness measurements. The reconstruction involves a tomographic inversion and solving the rate equations for the deuterium atom occupation density. Near term efforts will focus on optimizing and automating the reconstruction process to provide rough estimates on the pedestal particle source. Detailed SOL modeling using EDGE2D-EIRENE and AutoUEDGE is underway to understand the HFS-LFS fueling asymmetries as well as their dependence on the B_t direction.

References

[1] A. M. Rosenthal et al. *Review of Scientific Instruments* **92**, 3 (2021)
[2] F. M. Laggner et al. *Review of Scientific Instruments* **92**, 3 (2021)
[3] R. L. Boivin et al. *Review of Scientific Instruments* **72**, 1 (2001)
[4] A. W. Degeling et al. *Review of Scientific Instruments* **75**, 10 (2004)
[5] E. M. Hollmann et al. *Review of Scientific Instruments* **74**, 9 (2003)
[6] M. Bernert et al. *Rev Sci Instrum* **85**, 3 (2014)
[7] T. Odstrčil et al. *Review of Scientific Instruments* **87**, 12 (2016)
[8] R. K. Janev et al. *Atomic and plasma-material interaction data for fusion. V.4* (1993)
[9] D. P. Stotler et al. *Physics of Plasmas* **22**, 8 (2015)
[10] F. Scotti et al. *Nuclear Fusion* **61**, 3 (2021)

Acknowledgments

This material is based upon work supported by the U.S. Department of Energy, Office of Science, Office of Fusion Energy Sciences, using the DIII-D National Fusion Facility, a DOE Office of Science user facility, under Awards DE-AC02-09CH11466, DE-AC05-00OR22725, DE-FC02-04ER54698 and DE-SC0014264.